

Dark Matter Caustics

Simon D.M. White^{*}, Mark Vogelsberger[†]

Max-Planck Institut fuer Astrophysik, Karl-Schwarzschild Strasse 1, D-85748 Garching, Germany

Accepted ???. Received ???; in original form ???

ABSTRACT

Caustics are a generic feature of the nonlinear growth of structure in the dark matter distribution. If the dark matter were absolutely cold, its mass density would diverge at caustics, and the integrated annihilation probability would also diverge for individual particles participating in them. For realistic dark matter candidates, this behaviour is regularised by small but non-zero initial thermal velocities. We present a mathematical treatment of evolution from Hot, Warm or Cold Dark Matter initial conditions which can be directly implemented in cosmological N-body codes. It allows the identification of caustics and the estimation of their annihilation radiation in fully general simulations of structure formation.

Key words: dark matter, caustics, phase-space structure, dynamics, annihilation, N-body

1 INTRODUCTION

The idea that the dark matter might consist of a collisionless “gas” of weakly interacting, neutral particles was first published by Cowsik & McClelland (1973) and Szalay & Marx (1976), though earlier discussion can also be found in the textbook of Zel’dovich & Novikov (1971). These authors proposed neutrinos as a promising dark matter candidate, and a claimed measurement of the electron neutrino mass at very nearly the expected value (Lyubimov et al. 1981) led to a flurry of interest in neutrino-dominated, so-called “Hot Dark Matter” universes. This continued until detailed numerical simulations showed the predictions for low-redshift structure to be quite inconsistent with observation (White et al. 1983). Attention then shifted towards more exotic particle candidates for Warm or Cold Dark Matter (Pagels & Primack 1982; Peebles 1982).

If a cold collisionless gas evolves from near-uniform initial conditions under the influence of gravity, the nonlinear phases of growth generically involve caustics analogous to those formed when light propagates through a non-uniform medium. This connection was explored in some depth by Russian cosmologists interested in neutrino-dominated universes (Arnold et al. 1982; Zel’dovich et al. 1983). Caustics are also a very evident feature of the similarity solutions for cold spherical infall published by Fillmore & Goldreich (1984) and Bertschinger (1985). It was another 15 years, however, before Hogan (2001) realised that dark matter annihilation could be very substantially enhanced in such caustics. He showed that for absolutely cold dark matter the annihilation probability diverges logarithmically as a particle passes through a caustic, and that for realistic dark matter candidates this divergence is tamed by the small but finite initial thermal velocities

of the particles. He argued that the annihilation radiation from dark halos might be dominated by emission from caustics.

The first rigorous calculation of annihilation rates in caustics was carried out by Mohayaee & Shandarin (2006) for Bertschinger’s (1985) similarity solution. They found caustics to enhance the total annihilation flux substantially in the outer regions for plausible values of the initial dark matter velocity dispersion, but to be progressively less important at smaller radii. It is unclear whether either of these results will apply in general, since the behaviour of the similarity solution is strongly influenced by its spherical symmetry (which reduces its phase-space dimensionality from 6 to 2) and by its lack of small-scale structure.

In the present paper we present a theoretical treatment of the growth of structure which shows how the geodesic deviation equation can be used to follow local phase-space structure in a Lagrangian treatment of nonlinear evolution. This formalism is well suited for implementation in N-body simulation codes, allowing the annihilation signal from caustics to be treated in full generality provided numerical artifacts from discretisation and integration error can be kept under control. We have presented results from a first implementation of this scheme in Vogelsberger et al. (2008). A closely related but somewhat more complex scheme is described by Alard & Colombi (2005). Here we complement this work by giving a fuller description of the mathematics behind the approach, in particular of the regularisation of caustic densities by the finite velocity dispersion of the dark matter. In the next section we describe our idealisation of the initial conditions for structure formation in WIMP-dominated cosmologies. Section 3 then presents useful general results for nonlinear evolution from these initial conditions. These are used in section 4 to describe the evolution of the local phase-space structure, in particular of its projection onto configuration space, following individual particle trajectories. Caustic passages can be identified and the associated annihilation signal can be calculated explicitly. A final section discusses possible future uses of this approach.

^{*} swhite@mpa-garching.mpg.de

[†] vogelsma@mpa-garching.mpg.de

2 IDEALISED INITIAL CONDITIONS FOR STRUCTURE FORMATION

In the current standard paradigm for cosmological structure formation, the dark matter is assumed to be a weakly interacting massive particle which decoupled from all other matter and radiation fields at an early epoch, well before the universe became matter-dominated. Since this time, the dark matter has interacted with other components only through gravity. In most such models there is a period after the transition to matter-domination when density fluctuations in all components are linear on all scales, and the residual thermal velocities of the dark matter particles are small compared to the large-scale velocities induced by density inhomogeneities. In this paper we will take an idealised representation of this situation as the initial condition for later evolution of the dark matter distribution.

Thus we assume that at the initial time t_0 the phase-space density of dark matter particles can be written as

$$f(\underline{q}, \underline{p}, t_0) = \rho(t_0)/m_p (1 + \delta(\underline{q})) \mathcal{N}((\underline{p} - \underline{V}(\underline{q}))/\sigma), \quad (1)$$

where $\rho(t)$ is the (time-varying) mean mass density of dark matter, m_p is the dark matter particle mass, \underline{q} and \underline{p} are position and velocity at the initial time and will be used as Lagrangian coordinates labelling individual dark matter particles as they follow their trajectories, $\delta(\underline{q})$ is the initial linear overdensity at position \underline{q} , $\underline{V}(\underline{q})$ is the linear peculiar velocity at \underline{q} and, for growing mode linear perturbations in the matter-dominated regime, is related to $\delta(\underline{q})$ through

$$\underline{V}(\underline{q}) = \nabla \phi \quad \delta(\underline{q}) \propto \nabla^2 \phi, \quad (2)$$

where $\phi(\underline{q})$ is the gravitational potential generated by the linear fluctuation field, σ is the thermal velocity dispersion of the dark matter particles at the initial time, and \mathcal{N} denotes the standard normal distribution in three dimensions. Our assumption that the initial density field is linear implies that $\langle \delta^2 \rangle \ll 1$, while our assumption that the initial dark matter distribution is cold implies that $\sigma^2 \ll \langle |\underline{V}|^2 \rangle$. Note that the latter condition applies even in the hot dark matter cosmology, provided the initial time t_0 is taken sufficiently late.

In phase-space the dark matter is thus confined initially very close to the three-dimensional “sheet” $\underline{p} = \underline{V}(\underline{q})$ and, indeed, its distribution becomes exactly three-dimensional in the cold limit $\sigma \rightarrow 0$. The projection of this sheet onto configuration space (the three-density) is very nearly uniform. It proves useful to work in initial coordinates where the velocities at each point are taken relative to $\underline{V}(\underline{q})$. We therefore define

$$\underline{A}(\underline{q}, \underline{p}) = \underline{p} - \underline{V}(\underline{q}), \quad (3)$$

and we approximate the initial phase-space density of the dark matter as

$$f(\underline{q}, \underline{A}, t_0) = f_0 \mathcal{N}(\underline{A}/\sigma), \quad (4)$$

where we neglect the spatial modulation by the factor $(1 + \delta)$ so that $f_0 = \rho(t_0)/m_p$ and the phase-space density becomes independent of \underline{q} . Because \underline{V} is the gradient of a scalar field the second-rank tensor $\partial \underline{A} / \partial \underline{q}$ is symmetric and the transformation of variables $(\underline{q}, \underline{p}) \leftrightarrow (\underline{q}, \underline{A})$ is canonical (Binney & Tremaine 2008). This will be important below.

3 EVOLUTION OF THE DARK MATTER DISTRIBUTION

We will assume that dark matter particles interact purely gravitationally at all times of interest. Each then moves independently of the others subject only to the collective gravitational potential. Particle accelerations depend on position and time, but not on velocity, and trajectories can be derived from the time-dependent Hamiltonian of the system (e.g. Peebles 1980). The evolution of the dark matter distribution is thus a Hamiltonian flow. A thorough development of the properties of such flows can be found in Appendix D of Binney & Tremaine (2008). We characterise the phase-space position of a particle at time t by its position \underline{x} and its peculiar velocity \underline{v} . In a Hamiltonian flow, particle trajectories through phase-space never intersect, so we can write the phase-space position at time t as a unique and invertible function of the initial phase-space position, i.e.

$$\underline{x} \equiv \underline{x}(\underline{q}, \underline{p}, t), \quad \underline{v} \equiv \underline{v}(\underline{q}, \underline{p}, t)$$

with the well-defined inverse relation

$$\underline{q} \equiv \underline{q}(\underline{x}, \underline{v}, t), \quad \underline{p} \equiv \underline{p}(\underline{x}, \underline{v}, t).$$

This is a standard Hamiltonian map so the transformation $(\underline{q}, \underline{p}) \leftrightarrow (\underline{x}, \underline{v})$ which it defines is canonical, incompressible and symplectic (see Binney & Tremaine 2008, for the mathematical significance of these terms). As noted above, the transformation of variables $(\underline{q}, \underline{p}) \leftrightarrow (\underline{q}, \underline{A})$ is canonical, so we can restate the (canonical) relation between initial and final configurations as

$$\underline{x} \equiv \underline{x}(\underline{q}, \underline{A}, t), \quad \underline{v} \equiv \underline{v}(\underline{A}, \underline{p}, t)$$

with

$$\underline{q} \equiv \underline{q}(\underline{x}, \underline{v}, t), \quad \underline{A} \equiv \underline{A}(\underline{x}, \underline{v}, t).$$

This simplifies the description of our problem considerably.

The collisionless Boltzmann equation is an immediate consequence of the incompressibility (in 6-D) of Hamiltonian flows – phase-space density is conserved along every trajectory in the flow. Eq. (4) then provides a complete formal solution for the evolution of the phase-space density distribution of the dark matter distribution:

$$f(\underline{x}, \underline{v}, t) = f_0 \mathcal{N}(\underline{A}(\underline{x}, \underline{v}, t)/\sigma). \quad (5)$$

The maximum phase-space density at time t is f_0 , and this density is achieved everywhere on a 3-dimensional subspace defined implicitly by $\underline{A}(\underline{x}, \underline{v}, t) = 0$. Phase-space densities are only significantly different from zero at points which are sufficiently close to this subspace which we refer to below as the “central sheet” of the phase-space distribution. The geometry of this sheet is very simple at early times: its projection onto 3-space is (approximately) uniform and only one point of the sheet projects onto each \underline{x} -position. Non-linear evolution stretches and folds the sheet, but does not tear it. It can then pass through a given \underline{x} -position multiple times, producing a series of streams, each with a different velocity \underline{v} . Caustics arise on the boundaries between regions with different numbers of streams. Figure 1 illustrates this situation for an analogous 1-dimensional system.

It is important to realise that the solution of Eq. (5) depends *only* on the assumed initial condition and on the fact that the dark matter obeys the collisionless Boltzmann equation. Thus it holds in the absence of any symmetry and during strongly non-equilibrium phases of evolution. In addition, it does not assume the gravitational potential to be generated by the dark matter alone, so it is valid, for

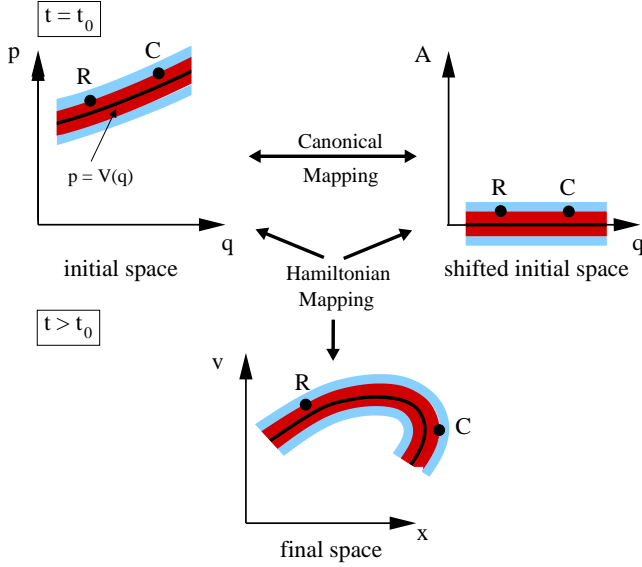


Figure 1. Illustration of our calculations for an analogous 1-dimensional system. At the initial time t_0 , the dark matter phase space density is non-zero only in regions of phase space close to the central sheet $p = V(q)$, indicated by the solid curve in the upper left diagram. The shaded regions surrounding this curve indicate the 1 and 2- σ regions of the (Gaussian) phase space density distribution. For convenience, we change the initial velocity coordinate in phase space to $A = p - V(q)$. As shown in the upper right diagram, the equidensity contours of the phase space density then correspond to $A = \text{const.}$, and the maximum phase space density occurs on the $A = 0$ axis. Dynamical evolution distorts these initial phase-space distributions according to the Hamiltonian flow $(q, p) \leftrightarrow (x, v)$, producing a phase space distribution at a later time t which is indicated schematically in the lower diagram. The collisionless Boltzmann equation guarantees that the phase space density is preserved by this map, as indicated by the shaded regions. Our plots indicate how two points R and C, corresponding to two different dark matter particles, are transformed by these maps. The (1-dimensional) space density in the neighborhood of each is given by projecting the phase space density down the velocity axis, and is uniform in the initial space. At time t , R is at a regular point of its trajectory ($\partial A / \partial v \neq 0$), whereas C is passing a caustic ($\partial A / \partial v = 0$). Clearly the space density at R depends on the local slope of its $A = \text{const.}$ line, while at C it depends on the curvature of this line and on the offset of C from the central sheet of its stream.

example, in the inner regions of galaxies, where the gravitational effects of the baryonic components are dominant. These influence the trajectories of individual dark matter particles, and so the details of $\underline{A}(\underline{x}, \underline{v}, t)$, but they do not affect the Hamiltonian nature of the flow or the validity of Eq. (5).

The Hamiltonian nature of the flow has a number of consequences for the map $(\underline{q}, \underline{A}) \leftrightarrow (\underline{x}, \underline{v})$. If we define 6-vectors $\overline{w} \equiv (\underline{q}, \underline{A})$ and $\overline{w} \equiv (\underline{x}, \underline{v})$, then the 6-tensors

$$\overline{\overline{D}} \equiv \frac{\partial \overline{W}}{\partial \overline{w}} \quad \text{and} \quad \overline{\overline{D}'} \equiv \frac{\partial \overline{w}}{\partial \overline{W}}$$

satisfy the relations

$$\overline{\overline{D}} \overline{\overline{D}'} = \overline{\overline{D}'} \overline{\overline{D}} = \overline{\overline{I}}, \quad \det(\overline{\overline{D}}) = \det(\overline{\overline{D}'}) = 1. \quad (6)$$

The first relation merely states that the backward transformation reverses the forward transformation, so the matrix corresponding to the former is the inverse of that corresponding to the latter. The second relation states that both matrices have unit determinant so that the transformations are volume- and orientation-preserving. The

conservation of phase-space density expressed by the collisionless Boltzmann equation is a consequence of this second property. Further important properties follow from the fact that these matrices are symplectic. In particular, the velocity and space parts of the forward and backward transformations are related by

$$\frac{\partial \underline{x}}{\partial \underline{q}} = \frac{\partial \underline{A}}{\partial \underline{v}}, \quad \frac{\partial \underline{x}}{\partial \underline{A}} = -\frac{\partial \underline{q}}{\partial \underline{v}}, \quad \frac{\partial \underline{v}}{\partial \underline{q}} = -\frac{\partial \underline{A}}{\partial \underline{x}}, \quad \frac{\partial \underline{v}}{\partial \underline{A}} = \frac{\partial \underline{q}}{\partial \underline{x}}, \quad (7)$$

where in each equation the partial derivative on the l.h.s. refers to the forward map so that the independent variables are \underline{q} and \underline{A} , while the partial derivative on the r.h.s. refers to the reverse map so that the independent variables are \underline{x} and \underline{v} . We will use some of these relations later.

4 VARIATION OF THE 3-DENSITY ALONG PARTICLE TRAJECTORIES

The differential annihilation probability for an individual dark matter particle depends on the (velocity-dependent) annihilation cross-section $\sigma_{\times}(v)$ and the local phase-space distribution as

$$\frac{dP}{dt}(\underline{x}, \underline{v}, t) = \int d^3 v' f(\underline{x}, \underline{v}', t) \sigma_{\times}(|\underline{v}' - \underline{v}|) |\underline{v}' - \underline{v}|. \quad (8)$$

In the following we will assume that $\sigma_{\times}(v) \propto 1/v$ as is the case for many (but not all) dark matter candidates. This relation then simplifies to

$$\frac{dP}{dt}(\underline{x}, \underline{v}, t) = \langle \sigma_{\times} v \rangle \int d^3 v' f(\underline{x}, \underline{v}', t) = \frac{\langle \sigma_{\times} v \rangle}{m_p} \rho(\underline{x}, t), \quad (9)$$

where $\rho(\underline{x}, t)$ is the local 3-space mass density of dark matter and $\langle \sigma_{\times} v \rangle$ is the thermally averaged velocity-weighted annihilation cross-section. The total annihilation probability over a finite time interval is thus simply obtained by integrating the local dark matter 3-density along the particle trajectory. This density is made up of two distinct components, one due to particles which are part of the same stream as the particle in question, and so were its neighbours in the initial conditions, and one due to particles in other streams, which typically originated in distant parts of phase-space. Caustics arise in the first of these two components and so we will concentrate on it in the following.

For our assumed initial condition, each particle can be specified by its initial phase-space position $(\underline{q}_p, \underline{A}_p)$, where $|\underline{A}_p| \sim \sigma$ is very small. Its later trajectory is then $\underline{x}_p(t) = \underline{x}(\underline{q}_p, \underline{A}_p, t)$, $\underline{v}_p(t) = \underline{v}(\underline{q}_p, \underline{A}_p, t)$, and the 3-space stream density at its position can be obtained by integrating the phase-space density over all velocities:

$$\rho_s(\underline{x}_p(t)) = \frac{f_0 m_p}{(2\pi\sigma^2)^{3/2}} \int d^3 v \exp\left(-\frac{|\underline{A}(\underline{x}_p, \underline{v}, t)|^2}{2\sigma^2}\right). \quad (10)$$

The velocity integral is restricted to velocities such that $\underline{q}(\underline{x}_p, \underline{v}, t)$ remains in the neighborhood of \underline{q}_p . Since σ is very small, we can simplify by carrying out a Taylor expansion of $\underline{A}(\underline{x}_p, \underline{v}, t)$ around $\underline{v} = \underline{v}_p$,

$$\underline{A}(\underline{x}_p, \underline{v}, t) = \underline{A}_p + \delta \underline{v} \frac{\partial \underline{A}}{\partial \underline{v}} + \frac{1}{2} \delta \underline{v} \frac{\partial^2 \underline{A}}{\partial \underline{v}^2} \delta \underline{v}^T, \quad (11)$$

where $\delta \underline{v} = \underline{v} - \underline{v}_p$ and the partial derivatives are evaluated at $(\underline{x}_p, \underline{v}_p)$.

4.1 Densities at regular points

At almost all points of the particle's trajectory the linear map in the second term on the r.h.s. of Eq. (11) is non-singular (i.e. the determinant of the corresponding matrix is non-zero). These will be called "regular points" of the trajectory in the following. At such points there exists a small value of $\delta \underline{v}$, say $\delta \underline{v}_c$, for which the sum of the first two terms vanishes; $(\underline{x}_p, \underline{v}_p + \delta \underline{v}_c)$ is then the intersection at time t of $\underline{x} = \underline{x}_p$ with the central sheet of the stream to which our particle belongs. The integral for $\rho_s(\underline{x}_p)$ becomes particularly simple if we centre the velocity integration on this point. To lowest order, we have

$$|\underline{A}|^2 = \delta \underline{v}' \frac{\partial \underline{A}}{\partial \underline{v}} \left(\frac{\partial \underline{A}}{\partial \underline{v}} \right)^T \delta \underline{v}'^T, \quad (12)$$

where $\delta \underline{v}' = \underline{v} - \underline{v}_p - \delta \underline{v}_c$. The tensor product $(\partial \underline{A} / \partial \underline{v})(\partial \underline{A} / \partial \underline{v})^T$ is clearly symmetric and must have positive eigen-values. Without loss of generality, let us define the principal axes in velocity space so that these eigen-values are $s_1^2 \geq s_2^2 \geq s_3^2 > 0$. The condition that our point be regular forces the final strict inequality, since an obvious consequence of Eq. (12) is

$$\det \left(\frac{\partial \underline{A}}{\partial \underline{v}} \right) = s_1 s_2 s_3. \quad (13)$$

In this velocity frame the integral in Eq. (10) takes a simple form which we can easily evaluate,

$$\begin{aligned} \rho_s(\underline{x}_p(t)) &= \frac{f_0 m_p}{(2\pi\sigma^2)^{3/2}} \int d^3 v \exp \left(-\frac{1}{2\sigma^2} \sum_{i=1}^3 s_i^2 \delta v_i'^2 \right) \quad (14) \\ &= \frac{f_0 m_p}{|s_1 s_2 s_3|} = f_0 m_p \left| \det \left(\frac{\partial \underline{A}}{\partial \underline{v}} \right) \right|^{-1} \\ &= f_0 m_p \left| \det \left(\frac{\partial \underline{x}}{\partial \underline{q}} \right) \right|^{-1}. \end{aligned}$$

The last equality follows from one of the relations listed in Eq. (7) and demonstrates explicitly that the stream density obtained here is identical to that obtained by forward integration of the geodesic deviation equation in Helmi & White (1999) and Vogelsberger et al. (2008). This is a manifestation of the fact that the local velocity distribution in a stream is distorted in a way which exactly mirrors that of the density field. To lowest order, the map rotates each infinitesimal Lagrangian volume and then stretches it by different amounts s_1 , s_2 and s_3 along three orthogonal axes. (Note that the s_i can be negative.) The (initially isotropic) velocity distribution at the central point is compressed by these same factors along the same set of axes.

4.2 Densities at caustic crossing

As a particle moves along its trajectory, it will occasionally pass through discrete points where the determinant of $\partial \underline{A} / \partial \underline{v}$ vanishes and the corresponding linear map becomes singular. At such points at least one (and generally only one) of the stretch factors must vanish, and Eq. (14) predicts an infinite stream density. These points are the caustics of the map. In the following we will neglect higher order singularities and assume $s_1^2 \geq s_2^2 > 0$, $s_3^2 = 0$ at such caustic crossings (see Tremaine 1999, for discussion of higher order singularities).

To simplify the integral in Eq. (10) it is useful to take coordinates in \underline{v} -space along the principal axes of $(\partial \underline{A} / \partial \underline{v})(\partial \underline{A} / \partial \underline{v})^T$. Unit vectors along the axes corresponding to s_1^2 and s_2^2 are rotated into a pair of orthogonal vectors in \underline{A} -space by the linear map

$\partial \underline{A} / \partial \underline{v}$, and in addition are stretched by factors s_1 and s_2 . We use these rotated directions to define our 1 and 2 axes in \underline{A} -space. All \underline{v} -vectors are then projected onto the 1-2 plane in \underline{A} -space. To lowest order, Eq. (11) becomes

$$\begin{aligned} \underline{A}(\underline{x}_p, \underline{v}, t) &= s_1 \delta v'_1 \underline{e}_1 + s_2 \delta v'_2 \underline{e}_2 \\ &+ \left(A_{p,3} + s_3 \delta v_3 + \frac{1}{2} \frac{\partial^2 A_3}{\partial v_3^2} \delta v_3^2 \right) \underline{e}_3, \quad (15) \end{aligned}$$

where the \underline{e}_i are unit vectors along the coordinate directions in \underline{A} -space. We have shifted the origin in \underline{v} -space in order to simplify the coefficients of \underline{e}_1 and \underline{e}_2 . By allowing the shift to depend on δv_3 , all terms independent of δv_1 and δv_2 can be removed; remaining second-order terms are then small compared to the linear term which is retained. A similar manipulation is not possible for the coefficient of \underline{e}_3 because its linear term vanishes at caustic crossing (i.e. $s_3 = 0$ when $t = t_c$) and we must retain both constant and quadratic terms. Note that the *only* quadratic term we need to retain is that involving δv_3 alone, since all others are subdominant to the linear terms involving $\delta v'_1$ and $\delta v'_2$ or are removed by the origin shift made for each value of δv_3 . Inserting this expression into Eq. (10) and setting $s_3 = 0$ (i.e. $t = t_c$), the integrals over v_1 and v_2 can be carried out as before and we are left with

$$\begin{aligned} \rho_s(\underline{x}_p(t_c)) &= \frac{f_0 m_p}{|s_1 s_2|} \frac{1}{(2\pi\sigma^2)^{1/2}} \\ &\times \int_{-\infty}^{+\infty} dv_3 \exp \left(-\frac{1}{2\sigma^2} \left(A_{p,3} + \frac{1}{2} \frac{\partial^2 A_3}{\partial v_3^2} \delta v_3^2 \right)^2 \right) \\ &= \frac{f_0 m_p}{|s_1 s_2|} \frac{\Gamma'(\pm |A_{p,3}|/\sigma)}{|\sigma \partial^2 A_3 / \partial v_3^2|^{1/2}} \exp(-A_{p,3}^2 / 2\sigma^2) \quad (16) \end{aligned}$$

where the dimensionless function Γ' is of order unity and is defined by

$$\Gamma'(X) = \frac{1}{(2\pi)^{1/2}} \int_{-\infty}^{+\infty} dy \exp(X^2/2 - (X + y^2/2)^2/2). \quad (17)$$

The sign of the argument of Γ' in Eq. (16) is positive when $A_{p,3}$ and $\partial^2 A_3 / \partial v_3^2$ have the same sign and negative otherwise. Note that Γ' can be expressed in terms of a modified Bessel function, but we forgo the details here.

As before, the mass density at the particle's position is related to the initial density $f_0 m_p$ by the product of three dilution/compression factors. The factors associated with the two axes in the plane of the caustic correspond to those we obtained above for regular points of the trajectory; caustic formation does not significantly effect the distortion of the dark matter distribution in directions parallel to the caustic. The compression/dilution in the direction perpendicular to the caustic is of different form, depending explicitly on how cold the initial conditions were (i.e. on the value of σ) and on how close the particle is to the central sheet of its stream (i.e. on the value of $A_{p,3}/\sigma$), as well as on the overall structure of the Hamiltonian flow, as encapsulated by the second derivative, $\partial^2 A_3 / \partial v_3^2(\underline{x}_p, \underline{v}_p, t_c)$. Note that as the initial conditions are made colder, the maximum density achieved during caustic passage increases as $\sigma^{-1/2}$.

For particles which lie away from the central sheet of the stream, $A_{p,3}$ is non-zero. If $A_{p,3}$ and $\partial^2 A_3 / \partial v_3^2$ have the same sign, the maximum of $\rho_s(\underline{x}_p(t))$ then occurs either slightly before or slightly after t_c . This is because a small but non-zero value of s_3 allows the linear term in the coefficient of \underline{e}_3 in Eq. (15) to be significant. For one particular s_3 the resulting quadratic has

an extremum at $A_3 = 0$. This value of s_3 obtains at the moment when our particle is spatially coincident with the caustic of the central sheet of its stream, and so sees the corresponding density (see Fig. 1). The exact value of the maximum density is not important in practice, since it appears only in the argument of a logarithm when we estimate the total annihilation radiation from caustic passages. For simplicity, we will set $A_{p,3} = 0$ when we use Eq. (16) below to estimate the maximum density during a caustic passage. In this case, Γ' can be expressed in terms of the standard complete Γ -function, $\Gamma'(0) = 2^{5/4}\Gamma(5/4)/\sqrt{\pi}$.

4.3 Integrating annihilation rates through caustics

The formalism developed above is particularly powerful when embedded in a high-resolution simulation of cosmic structure formation. Vogelsberger et al. (2008) showed how the geodesic deviation equation can be integrated in parallel with the N -body equations of motion to give the full phase-space distortion tensor $\overline{\overline{D}}$ along the trajectory of each simulation particle. This is then sufficient (through Eq. (7)) to give all the first order derivatives of the forward and backward Hamiltonian maps we have been discussing. In particular, this allows the local stream density to be calculated at all regular points of each trajectory using Eq. (14), and this can be inserted into Eq. (9) to obtain the intra-stream annihilation rate at such points.

Caustic crossings can be recognised in an N -body integration by the change in sign of the determinant of $\partial\underline{x}/\partial\underline{q}$. Let us denote by (s_1, s_2, s_3) and (s'_1, s'_2, s'_3) the stretch factors at the beginning and end of a timestep during which a caustic crossing is detected. Then $s_1 \approx s'_1$ and $s_2 \approx s'_2$, while s_3 and s'_3 should be much smaller in absolute magnitude and should have opposite sign. A good approximation to the evolution of the distortion tensor during the timestep is then obtained by assigning mean values to s_1 and s_2 and assuming s_3 to vary linearly between its endpoint values. According to the arguments of §4.2, the maximum value of ρ_s during the timestep is then well approximated as

$$\rho_{\max} = \frac{2^{5/4}\Gamma(5/4) f_0 m_p}{\sqrt{\pi} |\bar{s}_1 \bar{s}_2| |\sigma \partial^2 A_3 / \partial v_3^2|^{1/2}}. \quad (18)$$

Away from caustic crossing (but still within the timestep) Eq. (14) can be used to obtain ρ_s which then varies inversely with s_3 and so with $|t - t_c|$, the time to caustic crossing. This suggests the following approximation to the variation of stream density within the timestep:

$$\rho_s(\underline{x}_p(t)) = \frac{f_0 m_p \Delta t}{|\bar{s}_1 \bar{s}_2| |s_3 - s'_3|} \left((t - t_c)^2 + T^2 \right)^{-1/2}, \quad (19)$$

where Δt is the length of the timestep and T is chosen so that $\rho_s(\underline{x}_p(t_c)) = \rho_{\max}$. The shape of this function in the neighborhood of its maximum is chosen purely for convenience, but the wings and the maximum value itself are correct. If we integrate Eq. (9) over the timestep using this formula we obtain

$$\Delta P = \frac{\langle \sigma \times v \rangle f_0 \Delta t}{|\bar{s}_1 \bar{s}_2| |s_3 - s'_3|} \ln \left(\frac{2^{9/2}\Gamma(5/4)^2 |s_3 s'_3|}{\pi \sigma |\partial^2 A_3 / \partial v_3^2|} \right), \quad (20)$$

where we have used the fact that $T \ll \Delta t$ and, for simplicity, we have assumed that the caustic occurs well away from either end of the timestep. Since a single simulation particle represents many dark matter particles, ΔP must be multiplied by m_{sim}/m_p (where m_{sim} is the simulation particle mass) to obtain the total number of annihilation events.

The properties of the dark matter appear in Eq. (20) through

the annihilation cross-section, and through the parameter σ which appears in the argument of the logarithm. Thus we recover the result of Hogan (2001) that in the cold limit the annihilation luminosity of a caustic is logarithmically divergent. For given particle physics parameters, an integration of the N -body and geodesic deviation equations provides all the quantities needed to calculate ΔP for each caustic passage, with the important exception of the second derivative $\partial^2 A_3 / \partial v_3^2$. Since this quantity appears only in the argument of the logarithm, it is sufficient to estimate it to order of magnitude, provided the estimator chosen has no strong bias when averaged over many caustic passages.

The condition for caustic passage, $\det(\partial\underline{A}/\partial\underline{v}) = 0$ places no constraint on the values of the second derivatives, so we can estimate the size of a typical component of $\partial^2 \underline{A} / \partial \underline{v}^2$ from the available Galilean-invariant quantities. These are the components of the 6-dimensional distortion tensor $\overline{\overline{D}}$ and the particle acceleration \underline{a} . For example, we can note that $\underline{a}(\partial^2 \underline{A} / \partial \underline{v}^2)(\partial \underline{x} / \partial \underline{A})$ is dimensionless and is expected to be of order unity, so that the size of our desired component of the second derivative can be estimated as the inverse of the product of the r.m.s. sizes of the components of \underline{a} and of the components of $\partial \underline{x} / \partial \underline{A}$. This assumption can be checked in simple 1-dimensional cases, and we will give an example based on the similarity solution for spherical collisionless collapse in a future paper. In this case, at least, the estimate we advocate here works remarkably well.

5 DISCUSSION

In this paper we have developed the mathematical background to enable a relatively precise evaluation of the annihilation radiation from dark matter caustics in fully general simulations of the non-linear growth of structure. Our scheme allows the annihilation rate to be integrated along the trajectory of each simulation particle, including correctly the contributions from all the caustics in which it participates. Typically each particle experiences several such caustic passages in each orbit around the dark matter halo in which it resides (see Vogelsberger et al. 2008). In order to include correctly the annihilation rate between particles which are members of *different* streams, it is necessary to estimate a local coarse-grained density at the position of each particle, and to add in the contribution due to streams other than its own. This can be done, for example, using the SPH technique, since the smoothing this introduces does not bias the luminosity predicted from inter-stream annihilations. When a particle passes through a caustic occurring in a stream other than its own, the time-integrated annihilation probability is still correctly reproduced in the smoothed system.

By implementing these methods in high-resolution simulations of galaxy formation it should be possible to achieve a complete numerical description of the expected annihilation radiation, limited only by the ability to resolve the smallest collapsed clumps of dark matter. This latter limitation can be severe when attempting to predict the total annihilation radiation from a representative cosmological volume. For a standard supersymmetric neutralino, for example, the emission should be dominated by the smallest collapsed objects, with masses well below that of the Sun (e.g. Taylor & Silk 2003). Recent work has shown, however, that this problem is much less severe when predicting the observability of annihilation radiation from the Solar System, which lies just 8 kpc from the centre of the Milky Way (Springel et al. 2008). According to these authors, less than 3 percent of the dark matter within 100 kpc of the Galactic Centre should be in small lumps; almost all

the rest should be in extended streams of the kind discussed in this paper (see also Helmi & White 1999). They argue that the highest signal-to-noise for detecting the annihilation signal will be that of the smooth dark matter distribution in the inner few kiloparsecs of the Galaxy; small subhalos will be significantly more difficult to detect. Application of the techniques we have presented here should allow a rigorous evaluation of an important and previously unresolved issue: whether the emission structure of this smooth component is significantly modified by caustic emission. In addition, they will allow an assessment of the expected morphology and observability of outer caustics around external galaxies, most notably the Andromeda nebula.

The authors thank Stéphane Colombi, Craig Hogan, Roya Mohayaee and Volker Springel for helpful discussions.

REFERENCES

- Alard C., Colombi S., 2005, *MNRAS*, 359, 123
- Arnold V. I., Shandarin S. F., Zeldovich I. B., 1982, *Geophysical and Astrophysical Fluid Dynamics*, 20, 111
- Bertschinger E., 1985, *ApJS*, 58, 39
- Binney J., Tremaine S., 2008, *Galactic Dynamics: Second Edition*. Princeton University Press
- Cowsik R., McClelland J., 1973, *ApJ*, 180, 7
- Fillmore J. A., Goldreich P., 1984, *ApJ*, 281, 1
- Helmi A., White S. D. M., 1999, *MNRAS*, 307, 495
- Hogan C. J., 2001, *Phys. Rev. D*, 64, 063515
- Lyubimov V., Novikov E., Nozik V., Tret'yakov E., Kozik V., Myasoedov N., 1981, *Sov. Phys. - JETP*, 54, 616
- Mohayaee R., Shandarin S. F., 2006, *MNRAS*, 366, 1217
- Pagels H., Primack J. R., 1982, *Physical Review Letters*, 48, 223
- Peebles P. J. E., 1980, *The large-scale structure of the universe*. Princeton University Press
- Peebles P. J. E., 1982, *ApJ*, 263, L1
- Springel V., White S. D. M., Frenk C. S., Navarro J. F., Jenkins A., Vogelsberger M., Wang J., Ludlow A., Helmi A., 2008, *Nature* (in press)
- Szalay A. S., Marx G., 1976, *A&A*, 49, 437
- Taylor J. E., Silk J., 2003, *MNRAS*, 339, 505
- Tremaine S., 1999, *MNRAS*, 307, 877
- Vogelsberger M., White S. D. M., Helmi A., Springel V., 2008, *MNRAS*, 385, 236
- White S. D. M., Frenk C. S., Davis M., 1983, *ApJ*, 274, L1
- Zeldovich I. B., Mamaev A. V., Shandarin S. F., 1983, *Soviet Physics Uspekhi*, 139, 153
- Zel'dovich Y. B., Novikov I. D., 1971, *Relativistic Astrophysics: Stars and Relativity*. University of Chicago Press